to appear in International Review of Cell and Molecular Biology

Crowding, diffusion, and biochemical reactions

Contact information for author:

Matthias Weiss
Experimental Physics I
University of Bayreuth
Universitaetsstr. 30
D-95440 Bayreuth
Phone: +49 (0) 921 55 2500
Email: matthias.weiss@uni-bayreuth.de

Ms Length: ~14000, 4 figures

Keywords: diffusion; anomalous diffusion; subdiffusion; reactions; macromolecular crowding; fluorescence correlation spectroscopy; fluorescence recovery after photobleaching; fractal kinetics; diffusion-limited reactions

Abstract

Diffusion is the basic mode of transport for molecules in living cells. Diffusion leads to dispersion of individual molecules, but it also is the driving force behind biochemical reactions and pattern formation as diffusional motion mediates reactant encounters. Owing to macromolecular crowding in all cellular fluids and biomembranes, diffusion of molecules in cells is quite different from the motion observed in dilute solutions in a test tube. Hindered and anomalous diffusion are seen in cells, and biochemical reactions are affected by these. This review is intended to give an introduction and a brief overview about causes and consequences of crowding-induced diffusion anomalies and their impact on biochemical reactions.

1. Introduction

Cellular fluids are crowded with macromolecules. Indeed, the concentration of macromolecules in cytoplasm reaches up to 400mg/ml (Ellis and Minton, 2003). Also cellular membranes, i.e. two-dimensional fluids, are highly crowded (Engelman, 2005). Here, depending on the organelle, about 50,000 transmembrane proteins have been reported (Griffiths et al., 1984; Quinn et al., 1984), and peripheral membrane proteins make this crowded condition even worse. Proteins are therefore tightly packed into the cell with little recreation space. Recent computer simulations nicely illustrate this fact (McGuffee and Elcock, 2010). Although crowding is a hallmark of living matter, typical biochemical assays rather work at low protein concentrations in dilute solution. Yet, given the extraordinary dense and crowded environment in cells, it is questionable how much these assays can report in cellular biochemistry. One may even wonder if and how proteins can actually move and perform their function in living cells.

This review is intended to give a brief overview of phenomena associated with diffusion in crowded media, e.g. diffusion-limited reactions and anomalous diffusion. Focusing on these dynamic aspects, some steady-state considerations associated with crowding and excluded-volume interactions can only be touched on briefly. For a more extensive review on these aspects we refer the reader to (Zhou et al., 2008). Also, in an attempt to not overload the reader with mathematics on (anomalous) diffusion, several details have not been included here. The interested reader will find a comprehensive review on these aspects in (Hoefling and Franosch, 2013; Klafter and Sokolov, 2012).

This review is divided into three main chapters. In chapter 2, different mathematical descriptions of diffusional motion are recapitulated, and subsequently the concept of anomalous diffusion is introduced in some detail. While some mathematics is certainly needed for that, the intention was here to reduce formulas to an absolute minimum and rather describe the basic ideas. Chapter 3 is devoted to state-of-the-art approaches to quantify diffusional motion *in vivo*. Here, also experimental findings on crowding and (anomalous) diffusion are summarized. In chapter 4, an introduction to diffusion-limited reactions is given and shortcomings of these classical

considerations in the context of crowded systems are discussed, and recent results on crowding and diffusion-limited reactions are highlighted.

2. Diffusion and random walks

Any (bio)chemical reaction requires the educts to meet in order to form a product. While one may facilitate the reactants' encounter in a test tube by using magnetic stir bars, virtually all reactions in living cells rely on diffusion as a means of transport. Sometimes, diffusion only has to bridge short distances after molecular motors have supported traffic on larger length scales, yet the majority of cellular reactions depends entirely on diffusional motion. Elucidating cellular reactions therefore requires some knowledge about diffusion. The theoretical background of diffusion, however, is taught very differently in the different disciplines of natural sciences. This chapter is intended to review the basic concepts and mathematical framework of normal and anomalous diffusion in a way that also diffusion-driven reactions in crowded media, e.g. the cell's cytoplasm, can be understood. The mathematics used in this chapter is restricted to the minimum needed for a basic description to not overload the reader. More detailed and mathematically deeper introductions may be found, for example, in (Hoefling and Franosch, 2013).

The first subchapter focuses on the macroscopic, phenomenological theory of diffusion that was established in the 19th century. In this context, diffusion is viewed as a transport mechanism that leads to the equilibration of concentration gradients. This view is extended in the second subchapter, where a microscopic interpretation of diffusion as an unbiased, independent random walk of molecules is discussed. While these two subchapters only discuss normal Brownian diffusion, the third subchapter introduces the framework of anomalous diffusion in a broader context.

2.1 Diffusion as a macroscopic transport mechanism

Diffusion is a phenomenon that can be observed in every-day life. For example, if a drop of ink is carefully placed in water, one can observe a slow spreading of ink molecules until the entire water assumes a homogenous bluish color (cf. sketch in Fig. 1A). Performing such an experiment under well-controlled conditions, and evaluating the spatiotemporal evolution of the ink concentration, $c(\mathbf{r},t)$, yields a number of insights: (i) ink molecules seem to prefer leaving regions of high concentrations, (ii) concentration gradients vanish over time, (iii) equilibration becomes faster for higher temperatures, (iv) equilibration becomes slower for more viscous fluids, i.e. ink spreads slower in glycerol than in water.

The first observation states that the flux of ink, **J**, points downhill of the concentration gradient, i.e. $\mathbf{J} = -D\nabla c(\mathbf{r},t)$. Here, bold letters indicate three-dimensional vectors and ∇ denotes the first spatial derivative along x-, y-, and z-direction of space, respectively; the action of ∇ therefore creates a three-dimensional vector out of the scalar concentration profile c(**r**,t). The prefactor D has dimensions of an area per time, e.g. $\mu m^2/s$, and is called the 'diffusion constant'. The linear relation between flux and concentration gradients is known as Fick's first law and, as it stands, it is solely justified by its excellent description of experimental data. Owing to observations (iii) and (iv), one anticipates a relation $D \sim T/\eta$, where T is the (absolute) temperature and η is the viscosity of the fluid in which the ink spreads. Again, this is a purely empirical law that fits experimental observations; a justification for this relation will be given in the next subchapter.

In addition to Fick's first law, we know that ink molecules are not destroyed in this experiment but only move to a different location. This can be stated formally by the so-called continuity equation $\frac{\partial}{\partial t}c(\mathbf{r},t) = -\nabla\mathbf{J}$, which states that the concentration's temporal variation (left-hand side) is solely given by sources and sinks of the diffusional flux (right-hand side). Inserting now Fick's first law into the continuity equation yields the famous diffusion equation (also called Fick's second law):

$$\frac{\partial}{\partial t}c(\mathbf{r},t) = D\nabla^2 c(\mathbf{r},t) \qquad \text{Eq.(1)}$$

This equation states that the temporal evolution of the concentration (left-hand side) equals the second spatial derivative, i.e. the curvature, of the concentration profile c(**r**,t). Interestingly, this equation was known already in the early 19th century as Laplace's heat equation.

To understand the contents of the diffusion equation, we will restrict the discussion for simplicity to one dimension, say, along a coordinate x (cf. Fig. 1A). The diffusion equation then reads $\frac{\partial}{\partial t}c(x,t) = D\frac{\partial^2}{\partial x^2}c(x,t)$. We start now with an infinitely thin but very concentrated ink droplet at x=0, i.e. $c(x,t=0) = c_0\delta(x)$ in mathematical terms.

Plugging this initial concentration into the diffusion equation [Eq.(1)] yields for all times t>0 a Gaussian concentration profile $c(x,t) = c_0 \exp(-\frac{x^2}{4Dt}) / \sqrt{4\pi DT}$ (cf. Fig. 1B). The peak in the concentration profile at x=0 does not move in time, yet it becomes less pronounced as the width of the concentration profile grows with time. The squared width is nothing else but the Gaussian's variance, $MSD(t) = \int_{-\infty}^{\infty} x^2 c(x,t) dx = 2Dt$. The variance in this context is also called the *mean square displacement* (MSD) of the ink molecules and is illustrated in two ways in Figs. 1C,D.

The corresponding result for arbitrary dimensions is easily obtained in a very general form:

$$c(\mathbf{r},t) = \exp(-\frac{\mathbf{r}^2}{4Dt}) / (4\pi DT)^{\dim/2} \qquad \text{Eq.(2)}$$

and

$$MSD(t) = \int_{-\infty}^{\infty} \mathbf{r}^2 c(\mathbf{r},t) d^{\dim} r = 2Dt \times \dim \qquad \text{Eq.(3)}$$

Here, bold letters indicate vectors, e.g. in a one-, two-, or three-dimensional space for which dim=1,2,3. With these equations, macroscopic diffusion is well described and a material-specific diffusion constant D that describes the speed of gradient equilibration can be quantified.

While it is clear, that the diffusion equation seems to act on behalf of the second law of thermodynamics (maximizing entropy by spreading/mixing the ink), the microscopic driving force that seems to fuel the motion of ink particles away from areas with high concentrations remains elusive in this picture. In order to overcome this limitation, one needs to take on a statistical perspective for single particles that was pioneered by Boltzmann.

2.2 Diffusion as a random walk of molecules

In the late 19th century Ludwig Boltzmann introduced a more atomistic view to the natural sciences that aimed at explaining thermodynamic phenomena via the statistics of individual particles instead of continuous fields or concentrations. Against

all odds and severe criticism of famous colleagues he formulated the basis for what is known today as statistical physics. Seeking for microscopic interpretations of thermodynamic laws also brought diffusion back into focus. In one of his seminal papers in 1905, Albert Einstein gave the first consistent microscopic interpretation of Fick's laws including a microscopic derivation of the diffusion constant (Einstein, 1905). The major step in this article was the assumption that small particles in or near thermodynamic equilibrium will perform a random walk due to a finite temperature. Before diving into details, let us fill the concept of a random walk with some life.

Let us consider a drunkard on the way home after a pub-crawl. Having had too many beers, the person will stagger from lamppost to lamppost, forgetting instantly where he/she came from. The chances to go left or right therefore are equal, namely p=1-p=0.5. Having visited N lampposts in total, the distance that the person has walked to the right (measured in lampposts k) is given by a simple Binomial distribution: $P(N,k) = \binom{N}{k} p^k (1-p)^{N-k} = \frac{N!}{(N-k)!k!} p^N$. Replacing k by (N-k), one obtains the Binomial for the number of steps to the left. Since both expressions are identical for p=0.5, and as steps to the left have to be counted negative (going to the right being defined as the positive direction) the net movement of the drunkard is strictly zero. This is indeed a result one might have guessed already. Nevertheless, the drunkard has moved while aiming to get back home. This (unproductive) movement is captured by the second moment of the Binomial, i.e. the width of the distribution aka the mean square displacement (MSD): MSD(N)=2Np(1-p)=N/2. The squared excursion length of the drunkard therefore grows linearly with the number of visited lampposts, N. In this example, N reflects the time that has elapsed after the random walk had started. If the street is a long one, i.e. if the number of visited lampposts is very large, the Binomial distribution for the actual position of the drunkard converges towards a Gaussian due to the central limit theorem. It can therefore be written in the form $p(x,t) = \exp(-\frac{x^2}{4Dt}) / \sqrt{4\pi DT}$ with x denoting the distance from the starting point of the random walk (=pub), D being a microscopic diffusion coefficient, and t counting the elapsed time. The function p(x,t) is called a probability distribution function (PDF), and it states the probability of finding a particle (=the drunkard) at a locus between x

and x+dx at any given time t. Here, dx is an infinitesimal small step. Certainly, we can now extend this consideration to any dimension dim=1,2,3… :

$$p(\mathbf{r},t) = \exp(-\frac{\mathbf{r}^2}{4Dt})/(4\pi DT)^{dim/2} \qquad \text{Eq.(4)}$$

Looking at the PDF in Eq.(4), we see that it is identical to the solution of the diffusion equation in Eq.(2)! Hence, the PDF for a single particle that undergoes an unbiased random walk has the same shape as a spreading concentration profile c(**r**,t). As a consequence, the equation of motion for both quantities is the diffusion equation, Eq.(1). This fairly deep result states that the random walk of a single particle is representative for an ensemble of identical, non-interacting particles. In other words, if we follow a single representative particle over a long time, we get the same information about an ensemble as if we had monitored the ensemble itself. Many experimental approaches to quantify diffusion, e.g. single-particle tracking microscopy (cf. chapter 3), rely on this equivalence.

We can now state that the equilibration of concentration gradients is not a driven process, but it simply reflects a large collection of particles that undergo a random walk with the same starting point. Moreover, even after equilibration the motion of individual particles will not stop. But due to their homogenous distribution the same number of particles will move on average to the right as those going to the left.

In the above reasoning, we have tacitly expanded the drunkard's motion from a regular grid of lampposts to continuous space and time variables. To be more explicit on that, we could write down Newton's equation of motion for a single particle that is subject only to a randomly fluctuating force. This random force is analogous to the wish of the drunkard to move into a random direction. The choice of a random force that causes the random walk is justified by arguing that the diffusing particle is hit by thermally excited, much smaller solvent molecules (e.g. water molecules or lipids around a protein). Since there is many of them, these impacts will be uncorrelated and the net force is a random kick. Moreover, for objects smaller than a micrometer the fluid's Reynolds number is very small (even for water), i.e. all inertia terms can be neglected. The particle's motion is then given by the overdamped Langevin equation $d\mathbf{x}/dt = \xi(\mathbf{x},t)$, where ξ describes the random force that may depend on

time and the position of the particle. As a result of this stochastic differential equation one obtains single trajectories of a diffusing particle and the set of all these trajectories is described statistically via the diffusion equation. For illustration, representative random walks from a Langevin equation are superimposed to the density profile in Fig.1A.

Due to the link between Langevin and diffusion equation, the strength of the random force ξ needs to be related somehow to the diffusion constant. Moreover, the strength of the random kick needs to be related to temperature as higher temperatures excite the solvent molecules more. As a consequence, the diffusion constant has to be proportional to temperature. Indeed, Einstein first derived in 1905 that the diffusion coefficient can generally be written as $D=k_BT/\gamma$ (Einstein, 1905) with k_B being Boltzmann's constant, T the absolute temperature, and γ being the friction coefficient of the particle in the fluid. This equation is the basic version of a fluctuation-dissipation theorem, i.e. thermally induced fluctuations (described by D) are related to frictional forces that moving particles experience (friction γ). For a spherical particle, the well-known Stokes-Einstein relation is recovered, i.e. from $\gamma=6\pi\eta R$ one obtains $D=k_BT/6\pi\eta R$. Here, η is the fluid's viscosity, and R is the radius of the particle. With these insights, the experimental observation in the previous subchapter, $D\sim T/\eta$, is totally explained in terms of fundamental quantities. With that, diffusional motion has a proper basis that is fueled by first principles rather than empirical laws. In addition, the concept of a random walk is an intuitive picture for Brownian motion of individual molecules.

2.3 Anomalous diffusion

Having constructed a link between Fick's diffusion equation and random walks of individual molecules, one might ask now which types of random walks are compatible with the above theoretical construction. Clearly, we have assumed an unbiased movement, i.e. going left and right should be equally probable. Beyond that, one can show with mathematical rigor that normal Brownian diffusion is obtained, when the (symmetric) random walk has the following ingredients:

• Successive steps are uncorrelated (this is called a Markovian random walk)

- The probability distribution function of step lengths, $p(\Delta x)$, has finite mean and variance, i.e. $\int_{-\infty}^{\infty} x^n p(\Delta x) dx < \infty$ for n<3.
- The probability distribution function of waiting times, $p(\tau)$, between successive steps of length Δx has a finite mean and variance, i.e $\int_{-\infty}^{\infty} \tau^n p(\tau) d\tau < \infty$ for n<3

Under these conditions, the famous central limit theorem holds and the motion will be eventually normal Brownian diffusion. Breaking one of these rules typically yields diffusion anomalies that are the topic of this subchapter. Deeper mathematical details may be found, for example, in (Klafter and Sokolov, 2012).

One of the most straightforward extensions to a Brownian random walk is a violation of the Markovian assumption, i.e. successive steps are chosen to be correlated. If this is the case, the random walk is said to have a memory and the random force ξ in the Langevin equation "remembers" its action at previous time steps. This might influence the random walk in two ways: If successive steps are positively correlated, the random walk becomes persistent, whereas for anti-correlated steps an anti-persistent motion emerges. In the picture of our drunkard, the persistent random walk means that having gone to the right will bias the drunkard's decision to go to the right again in the next move. For an anti-persistent walk, the bias is just the opposite, i.e. having stepped left, the more likely decision of the drunkard is to take a step to the right at the next instant of time. In both cases, a few more beers may restore Markovian behavior…

Memory effects, however, massively impede finding a particle's PDF, i.e. the analogue to Eq.(4). To avoid nasty mathematical details, we will not dive into this realm. However, the width of the PDF, i.e. the mean square displacement MSD(t), is a pretty straightforward quantity that can already report on the characteristics of the diffusional motion. Depending on the type of memory, the MSD can show an anomalous power-law increase: $\mathrm{MSD}(t) = Kt^{\alpha}$ with $0 < \alpha \leq 2$. Here, K is a generalized diffusion coefficient with fractional units. The cases α=1 (normal diffusion with K=D, cf. previous subchapter) and α=2 (directed ballistic motion with velocity K=v) are trivial special cases. If α deviates from unity but is lower than two, one speaks of

anomalous diffusion to highlight the difference in the power-law increase with time. Here we can distinguish two regimes: If $\alpha<1$ the motion is called subdiffusion, whereas for $\alpha>1$ it is called superdiffusion.

For a correlated random walk, the most popular model is fractional Brownian motion that has been introduced by Mandelbrot in the 1960s (Mandelbrot and van Ness, 1968). The anomaly of fractional Brownian motion (from sub- to superdiffusion) can be tuned at will via the so-called Hurst coefficient $H=1-\alpha/2$, i.e. $0<H<1$. The model of fractional Brownian motion is particularly relevant for the case of subdiffusion ($\alpha<1$, $H>0.5$), where the anti-persistent, anti-correlated random walk can be related to the viscoelasticity of the fluid in which the particles diffuses (Ernst et al., 2012; Mason and Weitz, 1995).

Instead of introducing correlations in successive steps of the random walk, also the step length distribution and/or the waiting time distribution can be altered in such a way that an anomalous diffusion emerges. Letting the distribution of waiting times between successive steps compatible with normal diffusion but changing the step length distribution may lead to superdiffusion. If the variance and/or the mean of the step length distribution diverges, the distribution is said to be of Levy-type. Levy-stable distributions, introduced by Paul Levy in the early 20th century, are proper distribution functions that do not obey the central limit theorem, i.e. the sum of Levy-distributed random numbers is not a new random number that asymptotically follows a Gaussian distribution. A particular realization of a Levy distribution is the Cauchy distribution $p(\Delta x) = \frac{1}{\pi(1+\Delta x^2)}$ that is a properly normalized distribution of step lengths with diverging moments (infinite mean and variance). This type of step length distributions yields so-called Levy flights and the particle trajectories have a superdiffusive characteristics (Klafter et al., 1996). Superdiffusive behavior has been observed, for example, for diving whales/fish (Humphries et al., 2010; Sims et al., 2008) or in the context of human mobility (Brockmann et al., 2006; Gonzalez et al., 2008). Yet, in the context of cells, superdiffusion is not a tremendously relevant concept. Superficially, it might be observed as a consequence of transient ballistic motion on cytoskeletal filaments with intermittent periods of free diffusion. Taking a closer look reveals, however, that this example is simply the superposition of normal

diffusion and ballistic motion. Only the crossover region between a linear (diffusive) and a quadratic (ballistic) increase of the MSD in time mimics a non-trivial power-law on certain time scales.

More relevant in the context of cell biology are Levy distributions for the waiting times $p(\tau)$ between two steps that are drawn from a well-behaved step length distribution (e.g. a Gaussian). If already the mean of the waiting time distribution $p(\tau)$ diverges (e.g., when having a Cauchy-like distribution for waiting times), also very long residence times become very probable and the diffusive spreading of molecules seems to become slower and slower as time progresses; the whole system shows ageing. The asymptotic power-law behavior of $p(\tau)$ for large residence times enforces a so-called continuous time random walk (CTRW) for individual particles. As a consequence, the trajectory of the diffusing particle looks like that of a normally diffusing particle yet the time spent at each location can be extremely long. For an ensemble of particles, the CTRW induces a MSD that follows a subdiffusive characteristics, $MSD \sim t^{\alpha}$, and the choice of the waiting time distribution determines the anomaly degree α. Yet, compared to fractional Brownian motion, the CTRW is a particular model. As it conflicts with the central limit theorem, a single particle's trajectory is not representative any more for an ensemble. In fact, inspecting the MSD for a single particle yields normal diffusion (MSD~t) whereas the ensemble shows subdiffusion. This phenomenon, i.e. time-averaged and ensemble-averaged MSD are qualitatively and quantitatively different, is called weak ergodicity breaking (He et al., 2008; Lubelski et al., 2008). Hence, depending on the type of experiment, grossly different results may be observed. Some aspects of this peculiar phenomenon will be discussed in more detail in the context of experimental findings in the next chapter.

Last but not least in a set of models that are associated with anomalous diffusion are obstructed random walks. If a particle diffuses in a maze of immobile obstacles, and if the density of obstacles is sufficiently high, subdiffusion can be observed over extended time scales (Havlin and Benavraham, 1987). If obstacles are also mobile the anomaly may vanish (see, for example, discussion in (Malchus and Weiss, 2010)). The reason for anomalous diffusion in a course of dense obstacles is the

geometric shape of the still accessible space: If obstacles are placed randomly, a connected cluster of non-accessible sites will emerge at a critical density ρ_c, the so-called percolation threshold (Havlin and Benavraham, 1987). At (and near) to this concentration, the still accessible space has a fractal geometry, i.e. it looks like a self-similar arrangement of paths on smaller and smaller length scales (Bouchaud and Georges, 1990). Some more details of fractals will be discussed in chapter 4 and Fig. 4 in the context of fractal kinetics. Normal diffusion on a fractal has all signatures of anomalous diffusion, i.e. tracer particles will be seen to display subdiffusion while exploring the fractal. Yet, only at the percolation threshold an anomaly will be observed for all time scales. Below ρ_c a crossover to normal diffusion will be seen for large times (Bouchaud and Georges, 1990; Havlin and Benavraham, 1987) and the anomaly exponent α will eventually converge towards unity for normal diffusion. By the very nature of the obstruction process, α will depend on the dimensionality of the space in which the obstructed diffusion is taking place. For membranes (two dimensions), $\alpha \approx 0.69$, whereas in cytoplasm (three dimensions) $a \approx 0.55$ at the percolation threshold (Bouchaud and Georges, 1990). It is also worth noting that α does not smoothly interpolate between unity and the stated lower bounds. Strictly speaking, the anomaly is only well defined at the percolation threshold and only the transient nature of the subdiffusion in case of an obstacle density below ρ_c imitates a power-law increase of the MSD with an intermediate value of α for finite time scales (Hofling et al., 2006).

Having introduced different models for subdiffusion, one may ask now how they are related to biological samples. Obstructed diffusion, for example, might be expected if larger membrane structures like vesicles and endosomes try to diffuse through the cell's interior that is heavily decorated with cytoskeletal elements and intermediate filaments. On membranes, almost immobile protein complexes and adsorbed filaments may act as obstacles for small proteins. Fractional Brownian motion will reflect a viscoelastic characteristics of fluids due to its anti-persistent character: Any movement of a macromolecule in crowded fluids results in squeezing nearby macromolecules. These, however, will respond analogous to a compressed polymer, i.e. an entropic spring behavior will aim at restoring the old positions. Such a local elastic response will enforce a memory and hence the desired anti-persistence. A

CTRW on the other hand may be envisaged as a diffusive motion in an environment with many traps (Saxton, 1996). These traps will stop the diffusion intermittently and hence spreads the waiting times between periods of free diffusional motion, yet a few conceptual problems make this scenario rather unlikely (Saxton, 2007). The following chapter will pick up these considerations in the context of experimental approaches to quantify diffusion in vivo.

3. Quantifying diffusion in living cells

This chapter is intended to give an overview of light microscopy methods that are frequently used to assess transport in living cells. Here, the more theoretical concepts of the preceding chapter will be put into an experimental context. The first two subchapters focus on ensemble-based and single-particle based experimental approaches, respectively. Important insights on diffusional motion derived from these approaches are summarized in the third subchapter.

3.1 Ensemble methods

Probably the most popular technique for quantifying diffusive transport in living cells is fluorescence recovery after photobleaching (FRAP). Since its first realization in the late 1970s (Axelrod et al., 1976a; Axelrod et al., 1976b), a number of variants have been developed to match particular scientific problems, especially in cell biology (Lippincott-Schwartz et al., 2001).

Before explaining FRAP in some detail, let us briefly recall how fluorescent molecules like GFP can be excited, how they emit their fluorescence light, and how they can bleach. In its most basic form, a fluorescent molecule can be described as a three-level system (Fig. 2). An incoming photon, from an arc lamp or a laser, can excite an electron from the dye's ground state (S_0) to the first excited state (S_1) if its energy fits the energy gap between both states. The photon's energy is determined by its wavelength, $E \sim 1/\lambda$. Owing to the more complex structure of dyes as compared to single atoms, each of the states S_0 and S_1 is subdivided into many vibrational levels. Therefore, the absorption spectrum of a dye is not sharply peaked at a particular wavelength λ, but rather covers a certain range of wavelengths (470-500nm for GFP). After having been shifted to the excited state, the electron relaxes quickly via vibrational modes to the lowest excited state S_1. From here, the electron can decay back after some nanoseconds to the sublevels of the ground state S_0 via spontaneous emission of a fluorescence photon. Due to the energy loss when sliding down vibrational modes in the excited state, the emitted photon has a lower energy than the exciting photon; the fluorescence is red-shifted ('Stokes-shift'). GFP, for example, is excited by blue light (λ=490nm) and fluoresces in green (λ=515nm).

In addition to these two so-called singlet levels, a third state is important: the triplet state. This state is different in its total spin configuration and as dipole-transitions like $S_0 \leftrightarrow S_1$ do not flip spins, the excited electron should never reach the triplet level. Collisions with surrounding molecules and the complex internal modes of fluorescent dyes, however, enable the excited electron to fall into this unfavourable state when the dye has absorbed a photon. As a transition back to S_0 is quantum-mechanically forbidden, this triplet state can only relax via collisions with surrounding molecules. The lifetime of the triplet state is therefore much longer than that of the S_1 state. In combination with a collision, the triplet state will decay radiationless after 1-100μs to the ground state S_0. As a consequence, fluorescent dyes blink on short time scales. While being in the triplet state, the dye also can undergo an irreversible transition to a non-excitable state – the dye bleaches and remains dark. This irreversible bleaching is the basis for FRAP.

The concept of FRAP is straightforward (cf. Fig. 3A): Given a spatial distribution of fluorescently labelled particles, e.g. GFP-tagged proteins in the cytoplasm, one selects a region of interest (ROI) in which dye molecules are irreversible bleached by a short but intense illumination with the appropriate wavelength. The intense illumination will force the dyes to undergo many excitation/emission cycles (each taking a few nanoseconds). At each cycle, the triplet state, from where the dye can bleach, will be reached with a certain probability, and thanks to the vast quantity of cycles, many dyes in the ROI will be bleached. The emerging dark region is subsequently monitored with a much lower illumination intensity that does not lead to bleaching any more. If the bleached ROI recovers at least partially, one knows that an exchange with non-bleached regions has occurred. For example, the observed recovery can be due to diffusion, directed transport, or binding events. For the sake of brevity we will focus only on diffusion-driven recoveries and neglect the latter two possibilities.

Typical FRAP experiments require to choose a ROI, to take at least one pre-bleach image of it with low illumination power, to bleach it rapidly with very strong illumination power, and to monitor then the post-bleach images with low illumination settings again (cf. Fig.3A). The integral fluorescence of the ROI is the experimental

quantity that reports on the diffusion-driven exchange of bleached and non-bleached molecules. Since the diffusion constant D has dimensions of an area per time (see chapter 1.1), the spatial form of the bleached ROI is of crucial importance in this protocol. Knowing the shape of the ROI, one can analytically derive fitting functions for FRAP curves via the diffusion equation [Eq.(1)], and fitting these functions to experimental data allow one to determine D. A key step in deriving these fitting functions is an assumption about the fluorescence profile right after the bleaching, i.e. the profile seen in the first post-bleach image. Certain assumptions for the post-beach profile may lead to systematic errors (see below).

The most basic variant of FRAP utilizes a stationary Gaussian-shaped laser beam that illuminates a roughly cylindrical ROI throughout the thickness of the entire specimen, e.g. a cell. The diameter of the beam (typically a few 100nm) is dictated by the optical setup. The fitting function in this case can be calculated analytically and by varying parameters to match experimental data, one may determine the diffusion coefficient that has carried the observed recovery. Due to the small beam diameter, transport properties can be probed locally in cells and even binding reactions can be monitored with some accuracy (Berkovich et al., 2011).

Today, commonly confocal laser scanning microscopes (LSMs) are used for FRAP as they allow for choosing arbitrary ROI geometries. With an LSM, one obtains raster images of a specimen by moving the laser beam in a rectangular grid over the sample. Selecting a set of pixels that define the ROI and scanning them with much higher laser power allows for bleaching an (almost) arbitrary ROI. While the optical resolution is certainly still diffraction-limited (typically to roughly half of the wavelength), the distance between two pixels can be chosen as low as 10nm. Hence, an image (and also a ROI) can be massively oversampled to enhance the signal and/or the bleaching.

To obtain a reasonably simple fitting function for diffusion measurements, one typically restricts FRAP experiments to bleaching a line, a square, or a circle. Circular ROIs are very convenient for diffusion measurements, and an analytical fitting function for the fluorescence recovery is available (Soumpasis, 1983):

$F(t) = \exp\left(-\frac{w^2}{2Dt}\right) \times \left\{ I_0\left(\frac{w^2}{2Dt}\right) + I_1\left(\frac{w^2}{2Dt}\right) \right\}$. Here, w denotes the radius of the ROI (typically some μm); I_0 and I_1 are modified Bessel functions (Abramowitz and Stegun, 1970). This expression not only is a valuable one for fitting FRAP data of normal diffusion (cf. Fig.3), it can also be extended to report on subdiffusion. To this end, one simply replaces Dt in the above equation by Kt^{α}, where K is a generalized diffusion coefficient with units of an area per fractional time (Saxton, 2001).

A word of caution is needed, however, when fitting experimental data. While one assumes almost always a sharp, step-like transition of the fluorescence from the ROI to the rest of the specimen when deriving a fitting function, the finite time needed for bleaching invalidates this assumption. The bleach profile looks much smoother than step-like. To put it simply: Bleaching takes a finite time during which the diffusion does not stop, and the motion of dye molecules that have been bleached early will render the ROI somewhat wider than intended. Fitting experimental recovery data now with an analytical expression that does not take this into account will lead to a systematic, 2-5fold underestimation of the diffusion constant (Weiss, 2004). To cope with this problem, more sophisticated fitting approaches have been developed, e.g. by taking into account the actual fluorescence profile in the first post-bleach image (Goehring et al., 2010). Despite this source of uncertainty, FRAP has been employed successfully in many studies to estimate the diffusional mobility of proteins and larger structures (Lippincott-Schwartz et al., 2001).

An alternative to FRAP when aiming and quantifying diffusion coefficients is the use of fluorescence fluctuation techniques. Presumably the most prominent of these fluctuations techniques is fluorescence correlation spectroscopy (FCS) that was invented even before FRAP (Magde et al., 1972). Being half-way between ensemble and single-particle approaches, the concept of fluctuation spectroscopy experiments will be outlined by using FCS as an example. For more recent developments related to FCS, we would like to refer the reader to (Digman and Gratton, 2011).

While FCS was invented already in the early 1970s (Magde et al., 1972), the technique only became popular with the advent of modern confocal microscopy in

the mid 1990s (Rigler and Elson, 2001). The prime reason for this late application was the need for small optical volumes to make FCS robust and feasible for cell-biological applications. Technically, this could be achieved with the advent of robust confocal microscopes. In a nutshell, modern FCS setups monitor the mean dwell time τ_D of fluorescent particles in a femtoliter-sized confocal volume (Fig. 3B). The faster the diffusion (high D) the lower the measured mean dwell time in the focus. At the heart of FCS lies a noise analysis of fluorescence fluctuations: Whenever a particle enters the confocal volume it will contribute to the fluorescence, whereas the fluorescence drops slightly if a particle leaves the confocal volume. From the mean dwell time (typically about 500μs) and the radius of the confocal volume (typically 250nm, depending on the optics used in the setup), one can easily build a quantity that yields a rough estimate for the diffusion constant: $(250\text{nm})^2/500\mu\text{s}=125\mu\text{m}^2/\text{s}$. A more refined analysis shows that this crude estimate is correct up to a factor four (cf. below). The requirements for an FCS setup are hence just a confocal microscope and a fast, sensitive detector that counts the fluorescence photons that are emitted from particles in the focus (Fig. 3B).

To obtain quantitative insights into the diffusion coefficient and a potential anomaly of the diffusion, the crude estimate above is clearly insufficient. The fluorescence monitored by the detector can be split into a constant average fluorescence and fluctuations around this mean value: $F(t) = \langle F \rangle + f(t)$. Here, brackets denote a temporal average. When taking confocal images, one clearly seeks to maximize the mean so that the fluctuations f(t) become negligible and do not distort the quality of the image. For FCS, however, the strategy is opposite as one needs the fluctuations for evaluating the particles' diffusion. Therefore, FCS works best at low dye concentrations and in principle a single dye per confocal volume (i.e. a concentration of 1nM) is sufficient to obtain reliable results. Since particles are not tracked individually, FCS may be regarded as an on-average-single-molecule technique. The noise analysis is done by calculating the so-called autocorrelation function $C(\tau) = \langle F(t)F(t+\tau)\rangle / \langle F\rangle^2 - 1 = \langle f(t)f(t+\tau)\rangle / \langle F\rangle^2$. This definition states that one should calculate the average of all possible products $F(t)F(t+\tau)$ along the recorded time series (i.e. for all t) for a set of time lags τ. These average values depend by definition only on the lag time, τ. Dividing by the squared average fluorescence and

subtracting unity ensures that the autocorrelation function will decay to zero for large lag times and that the offset will be related to the number of particles in the focus. Essentially, $C(\tau)$ states the probability that a photon that has been recorded at time $t+\tau$ comes from the same dye as a photon that has been recorded at time t. Hence, if τ is extremely small, the photons will always come from the same dye molecules and $C(\tau)$ is larger than zero. In contrast, for large lag times all dye molecules that contributed to the fluorescence at time t have already diffused out of the confocal volume and another set of dyes sends out the photons. These photons are totally uncorrelated and thus $C(\tau)$ is zero for large τ. The interpolation between these two extremes, i.e. the typical time at which the correlation has dropped by 50%, yields the desired information about the type and kinetics of the diffusion.

Fitting curves can be obtained by bearing in mind, that the fluorescence is simply the sum of all fluorescence contributions from individual dyes in a given illumination profile $I(\mathbf{r})$, i.e. $F(t) = \int I(\mathbf{r})c(\mathbf{r},t)dV$. Here, the spatiotemporally varying concentration of particles $c(\mathbf{r},t)$ is included, that evolves in time according to the diffusion equation; integration runs over the entire space. In a confocal microscope the illumination profile (more correct: the superposition of illumination and detection profile) is a Gaussian of the form $I(\mathbf{r}) = I_0 \exp\left(-\frac{x^2+y^2+z^2/S^2}{r_0^2}\right)$. Typically, the beam radius is connected to the illumination wavelength as $r_0 \approx \lambda/2$. The elongation of the confocal volume by a factor S=3-5 along the optical axis is a feature of the usual optical path, in which only fluorescence in a half-space is detected while the fluorescence in the opposite half-space is lost. Inserting this expression into the definition of the autocorrelation function and splitting the concentration into a mean and a fluctuating part yields a double integral expression for $C(\tau)$. The argument of the integration is essentially the product of the Gaussian illumination profile and a correlator of the concentration fluctuations. The latter is nothing else but the propagator of the diffusion equation, namely the Gaussian PDF of Eq.(4) in the previous chapter! The whole calculation now reduces to evaluating two Gaussian integrals. The result for three dimensions finally reads: $C(\tau) = \frac{1/N}{1+\tau/\tau_D} \cdot \frac{1}{\sqrt{1+\tau/(S^2\tau_D)}}$; $\tau_D = \frac{r_0^2}{4D}$.

The offset of the correlation function thus reports of the inverse average number of particles in the focus, N, while the typical decay time τ_D reports on the inverse diffusion constant. Comparing this expression to the above crude estimate, only a factor four and a proper definition of the focus width have led to a slight update. Subdiffusion can be easily implemented into the above equation when replacing τ/τ_D by $(\tau/\tau_D)^\alpha$ (Weiss et al., 2004). While one may derive more elaborate fitting functions for anomalous diffusion (Lubelski and Klafter, 2009), the improvement of describing experimental data is typically smaller than the measurement error (Weiss et al., 2004). Hence, the simple exchange method (τ/τ_D replaced by $(\tau/\tau_D)^\alpha$ in the fit equation) yields a straightforward and easy procedure that captures the essence of the potential subdiffusion.

Using FCS one can determine diffusion constants on a local scale (within the focus) without perturbing or bleaching the cell. Unlike FRAP, where bleaching occurs along the optical axis throughout the whole cell, FCS also probes diffusion along the optical axis, albeit not very sensitively. Being an almost-single-molecule technique, the overexpression of proteins can also be held low in FCS experiments to not perturb the cell's native state. Yet, quantifying long-range diffusion beyond the focus is not possible. This can be cured, however, with techniques that use two foci (Dertinger et al., 2007) or whole images (Kolin and Wiseman, 2007) and still evaluate the fluctuations due to diffusion in a very similar manner as the approach for FCS.

3.2 Single-particle methods

A drawback with FRAP and even fluctuation methods like FCS is the lack of information about the individual trajectory of a diffusing particle. To put it differently, FRAP and FCS only yield the particles' mean square displacement. For subdiffusion, however, we have discussed in the previous chapter three very different models that can lead to the same nonlinear scaling of the MSD. Therefore, FCS and FRAP can hardly distinguish between such models. Tracking individual particles (even individual molecules) provides the maximum information as the whole trajectory is available after the measurement and not just its temporally changing variance.

In principle, tracking fluorescently labelled particles like quantum dots in two dimensions, e.g. on the cell's plasma membrane, only requires an epifluorescence microscope with a stable illumination source and a fast and sensitive camera for image acquisition. Often, an EM-CCD or a sCMOS camera are used, depending on the strength of the fluorescence signal and the required speed of acquisition. If the number of labeled particles is low and if the fluorescence background is not too strong, individual nanometer-sized particles can be detected easily with this setup. Although the particles are much smaller than the diffraction limit (i.e. the resolution limit of the optics), the position of the particle can be determined with nanometer precision. Simplifying the particle to a point-like source of fluorescence light, the particle will emit a characteristic pattern of light, the so-called point-spread function (PSF). The PSF states the probability that a fluorescence photon will be sent from the particle to a particular position on the detector (=the camera chip). For point-like particles the PSF image has almost a Gaussian shape. Fitting a Gaussian to the camera image of the tracked particle can be done with an accuracy that only depends on the number of photons that have been captured to image the PSF (Brauchle et al., 2009). For a high frame rate, only few photons contribute whereas lower frame rates yield a smoother image and therefore a better fit. The peak position of the Gaussian can be extracted via that approach with a few nanometer precision. In fact, the use of this simple trick also underlies modern superresolution microscopy techniques like PALM or STORM (Thompson et al., 2012).

A number of problems, however, make single particle tracking in cells a challenging project. First, GFP is prone to rapid bleaching, i.e. the number of positions in the tracking data is fairly limited. Therefore, one has to average the MSDs of many individual particles or one needs to employ more stable dyes. Second, cells show a strong fluorescent background that may mask individual particles. This is particularly problematic for blue/green variants of GFP; more red-shifted variants suffer less from background issues. Third, particles move while acquiring the photon for fitting the PSF image. This leads to an apparent superdiffusive behavior that may obscure the data evaluation (Goulian and Simon, 2000). Fourth, tracking in three dimensions, e.g. in cytoplasm, is challenging as the positional accuracy along the optical axis can be estimated less well. Moreover, one also needs to compensate for the z-motion to not loose the particle.

Despite these challenges, single-particle tracking has been frequently used to assess diffusion in cells. Owing to the full trajectory, one can also inspect additional quantities that go beyond the MSD. A particularly interesting quantity is the probability distribution of first passage times, i.e. the individual times that particles need to bridge a certain distance. These times are predicted to follow an inverse Gaussian law for normal diffusion (Klafter and Sokolov, 2012), yet to probe or exploit this distribution, a very large number of transit times needs to be recorded. A more robust measure is the asphericity of the diffusion track of individual particles. Counterintuitive to a naïve expectation, individual random walks are not spherical on average but assume an elliptical shape (Rudnick and Gaspari, 1987). The asphericity of this ellipsoid changes with the type of random walk and also with the dimension of the environment in which the diffusion takes place (e.g. bulk or on a surface). Since individual particles do not align their ellipsoidal walks, an ink droplet composed of many particles spreads symmetrically, i.e. in the ensemble our assumption of an isotropic random walk is fine again. As we shall see in the next chapter, (sub)diffusion can be characterized with the asphericity in much more detail as compared to FCS or FRAP experiments

3.3 Experimental results on diffusion in crowded media

Using the above techniques, the diffusive motion of cytoplasmic and membrane-bound proteins have been investigated in great detail. For the sake of brevity, we will restrict this chapter only to those phenomena that are associated with crowding.

In general, small cytosolic or nucleoplasmic proteins have been seen to diffuse with typical diffusion constants of about 20μm^2/s whereas membrane proteins are about 50fold less mobile (Dix and Verkman, 2008). Complex formation and/or interactions with larger structures certainly may slow down the apparent diffusion even more. However, from basic hydrodynamics and thermodynamics (Einstein-Stokes equation, cf. chapter 2.2), one can estimate the diffusion constant of small globular proteins (say, with a mass of 25kDa) to be in the range of 80μm^2/s in water or buffer solution. Using the Saffman-Delbruck relation (Saffman and Delbruck, 1975) one obtains for single-pass transmembrane proteins approximately 3μm^2/s. The strongly

reduced mobility observed in cellular environments as compared to these first-principle estimates is a first signature of crowding (Dix and Verkman, 2008). A plethora of dissolved macromolecules increases the apparent viscosity η of cellular fluids and membranes, which leads to a significant reduction of the diffusion coefficient. The change of viscosity from water to cytoplasm has been reported for many different cell types and conditions to be roughly 3-5fold, see e.g. (Elsner et al., 2003; Seksek et al., 1997). Hence, due to macromolecular crowding, diffusion is about 3-5fold slower in cytoplasm (and nucleoplasm) as compared to water or buffer solution. For diffusion on membranes, similarly strong reductions have been observed (Frick et al., 2007). As an additional note, we would like to highlight that diffusion constants on membranes in general have a peculiar size-dependence that strongly deviates from the commonly envisaged Einstein-Stokes law D~1/R in bulk fluids (R denoting the protein's hydrodynamic radius). For details, we refer the reader to the extensive literature on this aspect. Starting points may be, for example, (Guigas and Weiss, 2006; Hughes et al., 1982; Petrov and Schwille, 2008).

Going beyond a mere reduction of diffusion constants, the emergence of anomalous diffusion has been observed for protein-sized particles in the cytoplasm (Guigas et al., 2007a, b; Tolic-Norrelykke et al., 2004; Weiss et al., 2004) and nucleoplasm (Guigas et al., 2007a, b; Wachsmuth et al., 2000) of eukaryotes, in the cytoplasm of bacteria (Golding and Cox, 2006; Weber et al., 2010), and on membranes (Weigel et al., 2011; Weiss et al., 2003). Even cell extracts (Guigas et al., 2007b) and biomimetic artificial solutions (Banks and Fradin, 2005; Pan et al., 2009; Szymanski and Weiss, 2009) with different crowding agents have shown subdiffusion. Typically, the anomaly in cellular fluids was seen in the range $0.5 \leq \alpha \leq 0.7$ whereas artificial fluids and membranes rather showed $0.7 \leq \alpha \leq 0.9$.

It should be noted at this point that the observed subdiffusion is always a transient phenomenon that asymptotically converges towards normal diffusion. On length and time scales that are large enough, normal diffusion ought to be restored. Indeed, all subdiffusion models in chapter 2 are just mathematical constructs that assume, for example, that proteins can get trapped for an infinitely long time. Certainly this is unphysical, i.e. in all of these models exists a smallest and largest length/time scale

beyond which normal diffusion has to emerge. So far, all observations of subdiffusion in cells are linked to length and time scales below a few microns and a few seconds. Probing diffusion on larger scales, e.g. by large area FRAP, reveals normal Brownian motion yet with a much smaller diffusion coefficient than anticipated.

Linking experimental observations of subdiffusion to any of the above models is not easy as typically only the MSD can be evaluated, e.g. in FCS and FRAP experiments. Yet, this does not discriminate which type of random walk one has observed in the microscope. Several reports for subdiffusion on membranes are most consistent with a model of obstructed diffusion (percolation). Proteins and larger complexes are 'sieved' by more immobile structures, e.g. translocons (Malchus and Weiss, 2010), or membrane-adsorbed cytoskeletal filaments (Fujiwara et al., 2002; Tomishige and Kusumi, 1999). For subdiffusion in artificial solutions and the cytoplasm, fractional Brownian motion seems to be the most reasonable explanation. Indeed, single particle tracking has revealed a distinct asphericity of the subdiffusive random walk that is most consistent with fractional Brownian motion (Ernst et al., 2012). While a normal Brownian motion (α=1) with the theoretically predicted asphericity 4/7 was observed for purely viscous fluids, crowded fluids showed a significantly decreased anomaly value (α=0.8) and a lower asphericity. In comparison to computer simulations of CTRW, obstructed diffusion, and fractional Brownian motion, it turned out that this result was only compatible with fractional Brownian motion. In line with this result, the cytoplasm appears viscoelastic when shearing it with high frequencies, i.e. the complex shear modulus has equally strong viscous and elastic contributions (Guigas et al., 2007a, b; Tseng et al., 2002; Yamada et al., 2000). Viscoelasticity of the crowded cytoplasm therefore can be seen to induce anomalous diffusion and the deformation memory induced by the elastic part is the cause for proteins to undertake a fractional Brownian walk. This very feature can dramatically alter biochemical reactions as we shall see in the next chapter.

4. Diffusion as a driving force for biochemical reactions

This chapter is intended to give an overview of the impact of diffusion on the progress of biochemical reactions. In the first subchapter, classical results on diffusion-driven reactions and limitations in these approaches are reviewed. In this context, also the impact of the reaction space's dimensionality on the progress and outcome of (bio)chemical reactions will be discussed. The second subchapter summarizes recent findings on biochemical reactions in crowded systems and the role of (anomalous) diffusion in this context.

4.1 Diffusion-controlled reactions

Virtually all biochemical reactions in a cell rely on diffusion. Reactions may be dissected into two phases with distinct time scales, and in each of these phases random walks are needed to drive molecular association. First, reactants need to undergo a diffusive search to come into close contact ('encounter phase'). If two cytosolic molecules with diffusion constants D_1 and D_2 that wish to react with each other are separated by a distance *s*, the typical time for their encounter is determined by the mean square displacement, i.e. $\tau = s^2/[6(D_1+D_2)]$. The sum of diffusion constants appears here since the particles need to move relative to each other and not just with respect to an immobile reference point for which the individual diffusion constant is the appropriate quantity. Diffusion coefficients therefore determine the time for complex formation of two (or more) molecules. In fact, as diffusion is a random walk, the typical encounter time τ only is the first moment (i.e. the mean) of a distribution of encounter times that is given by an inverse Gaussian. Once two molecules are in close proximity, the second phase of a reaction can proceed. Molecules reorient by rotational diffusion until the binding sites of both reactants face each other. At this point a small lateral diffusion step downhill the binding potential finalizes the binding event and leads to a lock-key type of arrangement.

Let us focus in the remainder to reactions that are limited by the first phase, i.e. by the encounter time. These reactions are named diffusion-limited since the search process dominates the time needed for a reaction. For the case of two molecules that wish to undergo a reaction in bulk fluid but are present only in minor amounts, Smoluchowski has derived already in 1916 an analytical expression for the reaction

constant in terms of the diffusion constants (Smoluchowski, 1916): Let us consider the basic reaction A+B->C between two species; the reaction rate is k. For simplicity, we assume that the reaction occurs rapidly after the molecules have met each other. If the two reactants A and B have radii r_A and r_B, and diffusion coefficients D_A and D_B, respectively, one can analytically calculate via the diffusion equation that $k = 4\pi(D_A + D_B)(r_A + r_B)$. Again, the sum of both diffusion constants reflects the relative motion of two diffusing particles. On can extend this result to include also the second phase of binding, i.e. when reactants need some additional time to bind after having encountered each other: $1/k = 1/\{4\pi(D_A + D_B)(r_A + r_B)\} + 1/\kappa$ with κ being the second order rate constant. The total reaction rate is hence the inverse sum of the times needed for encountering and reacting.

Smoluchowski's construction seems to yield an elegant solution for considering diffusional motion in reactions. However, it relies critically on the assumption that molecules move in a three-dimensional fluid. If molecules move in one or two dimensions, e.g. on a membrane or on a cytoskeletal filament, the construction fails and an analytical expression for a reaction constant cannot be derived any more. Indeed, the situation is even worse: The reaction coefficient is not a constant any more but depends on time! The reason for this counterintuitive phenomenon is based on the geometrical properties of the molecules' random walk as compared to the space in which they move. In brief, a random walk is a two-dimensional object by its very construction and Smoluchowski's construction only is valid when reactants perform a random walk in an environment that has a dimension larger than two (e.g. in a three-dimensional bulk fluid). The next paragraph will give a more concise explanation of this statement.

In order to understand why a random walk's geometry is important, we need to briefly reflect on the definition of the term 'dimension'. Our intuition is compatible with Euklid's definition of dimension. Points, lines, surfaces, and volumes are zero-, one-, two-, and three-dimensional objects, respectively. Yet, in the 1960s a new definition of so-called 'fractal' dimensions was introduced (Mandelbrot, 1983) that triggered not only a heap of scientific work but also inspired artists (just search the internet for a visualization of the Mandelbrot set). To understand the concept of a fractal

dimension, let us imagine an arbitrary object whose dimensions we wish to determine, say, a wiggly line on a flat piece of paper (cf. Fig. 4). If we superimpose a square grid with mesh length ε onto the paper, we can determine the number of tiles that are visited by the line, $N(\varepsilon)$. We then iteratively refine the mesh by decreasing ε and count again. Having done so many times, the number of tiles that touch the line for a given mesh size ε shows a scaling $N(\varepsilon) \sim 1/\varepsilon^{d0}$ for small box sizes ε (Fig. 4). The exponent d_0 is called the fractal dimension (more precisely, it is named the box-counting dimension), and it agrees with our intuitive Euklidian definition: For points $d_0=0$, for lines $d_0=1$ and so on. The value of d_0, however, does not have to assume integer values. If the wiggly line is the so-called Koch curve (cf. Fig. 4) the fractal dimension is $d_0 \approx 1.26$. This curve is therefore neither a line nor a surface; it is something in between. Indeed, zooming into the curve, it seems to repeat itself on smaller and smaller length scales. This self-similarity is the hallmark of fractals and one measure for the self-similarity is the fractal dimension d_0.

A box-counting procedure for a protein's random walk in buffer solution yields the fractal dimension of normal Brownian diffusion: $d_0=2$. Normal diffusion is therefore filling a surface but not a three-dimensional volume. This property of "filling" an environment or not is captured by the term 'compact' vs. 'non-compact' random walk. Diffusion is a compact random walk on a membrane but not in three-dimensional cytoplasm. With this insight, we can now see a deeper reason why Smoluchowski's construction does not work in one or two dimensions: The random walk is compact. One can only define a reaction constant if diffusion is non-compact, otherwise the reaction rate k depends on time (Benichou et al., 2010). This is particularly important for diffusion in two dimensions (e.g. for proteins in the plasma membrane) but also for subdiffusion in cytoplasm. If proteins are subject to fractional Brownian motion, i.e. if they show crowding-induced subdiffusion in a viscoelastic fluid (cf. chapter 3), the random walk takes on a fractal dimension $d_0=2/\alpha$. Subdiffusion therefore can be a compact random walk in three dimensions (for $\alpha<2/3$, i.e for values that have been experimentally observed, cf. chapter 3). In this case Smoluchowski's approach fails even for reactions in bulk fluids and one cannot define a proper reaction constant any more. These reactions are said to be fractal or fractional and consequences for biology will be discussed in the next subchapter.

4.2 Target finding, rebinding, and enzymatic reactions in crowded media

From the above it is clear that understanding biochemical reactions in crowded cellular fluids requires some knowledge about diffusive transport and its potential anomalies. Especially reactions that rely on few molecules (say, a couple of thousands per cell, i.e. at nanomolar concentrations and below) are particularly affected by properties of diffusive transport as these reactions are diffusion-limited.

General approaches to describe biochemical reactions, e.g. in many systems biology approaches (Kholodenko, 2006), are based on the law of mass action and sets of ordinary differential equations (ODEs). A prominent example is the Michaelis-Menten reaction $E + S \leftrightarrow C \rightarrow E + P$ in which an enzyme E can reversibly form a complex C with its substrate (S). Alternatively to falling apart, the substrate/enzyme complex can progress to a product P and the unconsumed enzyme. This chemical equation can be translated to a set of ODEs for the reactants' concentration. In this approach, well-mixed conditions are assumed for all times, and reaction coefficients include diffusional motion of molecules only via the Smoluchowski construction (cf. previous subchapter). Such an approach, however, may be problematic. First, if the number of involved particles is small, a concentration may not be a good description in the first place: If there are just 1000 substrate molecules to be modified in a cell of volume $1000\mu m^3$, the concentration of unmodified substrates can only assume discrete values between 1.6nM (max) and 0.0016nM (min). Any value below the lower bound is strictly zero, i.e. there is simply no particle left to be modified. Yet, in an ODE system this lower bound is typically not considered. Second, assuming well-mixed conditions implies that substrate and enzyme will immediately take on a nonzero equilibrium distance when dissociating from each other without product formation. In better words, rebinding of the same enzyme molecule to the substrate is as likely as binding a completely different enzyme molecule. This can only hold true for high enzyme concentrations, say, above ~100μM. Third, the dimension in which particles have to search for each other matters (cf. above), i.e. the Smoluchowski construction may not be valid at all. Finally, an ODE formulation implies that diffusion can be described by a single time scale, namely the ratio of the squared typical distance

between reactants and the sum of diffusion constants. Yet, in the presence of anomalous diffusion, multiple time scales are involved in the diffusional motion.

Several lines of evidence have recently supported these fairly general caveats. The first two criticisms are highlighted, for example, in a particle-based simulation of the MAPK signalling pathway (Takahashi et al., 2010). Unlike ODEs, these stochastic simulations include naturally rebinding events of just released enzyme molecules via an event-based algorithm. With this approach, the authors were able to show that the commonly assumed bistability of the MAPK pathway (Markevich et al., 2004) is an artifact of the widely used ODE description. For physiological concentrations of MAPK and its kinase, rebinding is of major importance. This result indeed challenges a fair number of ODE-based systems biology studies.

When considering subdiffusion of the fractional Brownian motion type, simulations also showed that product formation in multi-phosphorylation cascades can be massively enhanced as compared to normal diffusion (Hellmann et al., 2012). In terms of the MAPK example this means that subdiffusion strongly enhances rebinding of MAPK kinases and therefore increases the yield of double-phosphorylated MAPK. Indeed, crowding-induced subdiffusion may allow for a continuous transition between a processive and a distributive kinase action: While a distributive kinase will dissociate from its substrate after having performed the first phosphorylation, subdiffusion strongly counteracts a diffusion-driven separation of the reactants and leads to a fast rebinding. Therefore it seems as if the kinase is processive, i.e. it stays bound to the substrate until all phosphorylations have been done. Thus, naming a kinase processive or distributive depends on the viscoelastic properties of the surrounding fluid. Indeed, strong changes of MAPK phosphorylation have been found when comparing crowded and non-crowded buffer conditions (Aokia et al., 2011).

Single-step Michaelis-Menten kinetics has also been studied numerically for obstructed diffusion in two dimensions (Berry, 2002). Here, enzyme and substrate were assumed to perform subdiffusion due to a percolation cluster of obstacles. In line with previous reports on fractal substrates (Kopelman, 1988), a fractal/fractional kinetics has been observed in this cases. A description via heuristic ODEs was only

possible for certain time scales. These observations are in line with simple reactions on a percolation cluster, where encounter and reaction have been probed separately (Saxton, 2002). Again, enhanced rebinding due to subdiffusion has been found in this case.

Simulations of subdiffusion on membranes also revealed reactant segregation (Hellmann et al., 2011). Since normal diffusion and subdiffusion are compact random walks in two-dimensional environments, reactant segregation (the so-called Zeldovich effect) is expected (Kopelman, 1988). In this case, reactions only occur at the interface between regions that are enriched in complementary reactants and a chemical structuring of the surface is observed. Also the formation of Turing patterns, which have been implicated in many cell-biological and developmental processes (Meinhardt, 1982), are strongly facilitated by subdiffusion (Weiss, 2003). Since the emergence of Turing patterns critically relies on strongly different diffusional mobilities of two counteracting reactants (typically named ‘activator’ and ‘inhibitor’), subdiffusion can massively enhance the stability of emerging patterns. In both of these situations, (sub)diffusion is a bad mixing strategy and domain formation may occur from local heterogeneities. Membrane domain formation in cell biology therefore may be just a reflection of the particularly bad diffusive mixing, and cells may have turned this into an advantageous strategy to foster signaling and mass exchange at particular spots.

While the above examples have been focused on certain classes of reactions, e.g. of the Michaelis-Menten type, the general problem of finding a target (say, a repressor aiming to bind at a certain DNA operon) is also strongly affected by the properties of diffusion. A classical result on this is the so-called ‘reduction of dimension mechansim’ for the Lac repressor (Berg et al., 1981). Given that there are only about ten copies of the repressor in each *E. coli* cell, one may ask how these few molecules can search and bind a single DNA operon in a short time. Diffusion through the cell’s cytoplasm and once in a while hitting the DNA at a random location is surely a bad search strategy. On the other hand, diffusing only along the DNA is by far too slow. Switching between these two extremes, however, massively improves the searching. Diffusion through cytoplasm and binding to a random piece

of the DNA followed by a brief sliding along the DNA in the neighborhood of the attachment point yields a fast and reliable search strategy (Berg et al., 1981). When two soluble proteins need to find each other in cytoplasm, however, reduction of dimension is in most cases not an option. Yet, if the particles are subject to subdiffusion (fractional Brownian motion), their random walk is a fractal with dimensions $d_0=2/\alpha$. If the anomaly is below 2/3, subdiffusion becomes a compact random walk and all points in space will be visited repeatedly. Hence, proteins will be able to find each other with a high probability. Indeed, simulations have shown that the probability of finding a target is massively enhanced for a subdiffusive search strategy albeit the diffusion process is slower than normal diffusion (Guigas and Weiss, 2008). Subdiffusion therefore does not speed up a search process but it makes it more reliable, i.e. proteins find their binding partners with a higher probability. If a cellular response does not have to occur too rapidly but requires a high degree of reliability, subdiffusive searching may be advantageous for cells.

Most of the above mentioned results have been found in numerical approaches. Experiments that probe specifically the influence of (sub)diffusion on biochemical reactions are still rare. The formation of complexes in crowded environments, e.g. amyloid fibre formation, has been studied in some detail. However, most of the measurements and interpretations have been focused on the effect of excluded volume in crowded solutions (see (Zhou et al., 2008) for an extensive review). Owing to more complex experiments, the contributions of (sub)diffusion have been studied much less. In a very recent study, we have been able to show that subdiffusion indeed can facilitate complex formation (Stiehl and Weiss, 2013). Here, the opening/closing of a ssDNA hairpin in artificial crowded solutions was studied via FCS. As a result of crowding and subdiffusion, an enhanced fraction of closed ssDNA hairpins was observed which matches well to the predictions of numerical simulations. It will be interesting to further extend these approaches to more complex biochemical reactions, e.g. signaling cascades in bulk and on membranes.

5. Concluding Remarks

Despite the fact that diffusion has been studied intensively for more than 100 years, its impact in the secret life of a cell is still far from being well understood. This review

has only highlighted a few ideas and problems in this context that hopefully will stimulate other researchers to consider transport properties more thoroughly when aiming at an understanding of complex biochemical reactions. Having identified important players of cell biology via many omics-approaches in the last decade, it is now about time to dive into the realm of quantitative biology that uses these molecular players together with concepts from physics in order to understand cellular organization and dynamics in detail.

Figure 1

Diffusion in a nutshell. **(A)** Diffusively spreading ink droplet at some instant of time seen from top. While the darkish center of the bluish contour plot indicates a still high concentration at the initial point of injection, also remote regions have assumed a light blue colour. Three representative random walks of individual ink molecules are superimposed in red, green, and orange. **(B)** Gaussian concentration profiles of the ink, c(x,t), along the dash-dotted line shown in (A). The more time has elapsed since placing the ink droplet in water (black to blue to green curves), the wider is the Gaussian and the lower is the concentration of the ink at the injection point (dashed red line). **(C)** The width of the Gaussian distribution shown in (B) is characterized by the mean square displacement (MSD). Normal Brownian diffusion shows a linear scaling MSD~t (black line), whereas sub- and superdiffusion (green and blue curves, respectively) show a power-law increase MSD~ t^{α} with $\alpha<1$ and $\alpha>1$, respectively. **(D)** The power-law increase shown in (B) is highlighted in a double-logarithmic plot.

Figure 2

Fundamentals of photophysics. A fluorescent dye, e.g. GFP, can be excited by a photon with the appropriate wavelength, i.e. an electron is shifted from the ground state S_0 to the excited state S_1 (blue arrow). In the excited state, the electron can relax via vibrational sublevels to the edge of the excited state (black arrow). From there, the electron can decay back to the ground state by emitting a red-shifted photon (green arrow). Alternatively, the electron may reach the triplet state T from the excited state S_1 (red arrow). From this state the electron cannot relax back to the ground state by sending out a fluorescence photon any more. Instead, the electron needs to relax via collisions (orange arrow). From the triplet state, the dye may also get irreversibly bleached. While this is unfavorable for FCS, it is the basis for FRAP experiments.

Figure 3

Principle of FRAP and FCS experiments. **(A)** Sketch of a pre-bleach and a post-bleach image of a GFP-expressing cell with a circular region of interest (ROI). After bleaching, the diffusion-driven recovery from unbleached regions to the bleached ROI is monitored with low illumination intensities (third sketch). The total fluorescence F(t) of the ROI starting at the first post-bleach image rises and eventually saturates to a steady state. Fitting the curve with theoretical expressions yields the diffusion coefficient. **(B)** In FCS, only the fluctuating fluorescence F(t) in a confocal volume is monitored as fluorescent particles go in and out of the illuminated focus. The autocorrelation function of these fluctuations decays sigmoidally in a semilogarithmic plot, and the half-time of this decay reports on the diffusion coefficient and the type of diffusion. See main text for details.

Figure 4

Fractal dimension of random walks. Representative Brownian random walk (blue) as compared to the famous fractal Koch curve (black). The strict self-similarity of the Koch curve is highlighted by zooming into the red region (magnification of the curve shown in red). Superimposing quadratic grids of different sizes ε (shown here as a grey box with a refined black mesh of 9 boxes) allows for quantifying the fractal dimension d_0 of both curves. The number of boxes that touch one of the curves, $N(\varepsilon)$, shows a power law decay $N(\varepsilon) \sim 1/\varepsilon^{d0}$. For small box sizes, an exponent $d_0=1.26$ is found for the Koch curve and $d_0=2$ for the Brownian random walk. Hence, a random walk is plane-filling while the Koch curve is something between a line and a surface.

References

Abramowitz, M., Stegun, I.A., 1970. Handbook of mathematical functions : with formulas, graphs, and mathematical tables. Dover, New York.

Aokia, K., Yamada, M., Kunida, K., Yasuda, S., Matsuda, M., 2011. Processive phosphorylation of ERK MAP kinase in mammalian cells. Proceedings of the National Academy of Sciences of the United States of America 108, 12675-12680.

Axelrod, D., Koppel, D.E., Schlessinger, J., Elson, E., Webb, W.W., 1976a. Mobility Measurement by Analysis of Fluorescence Photobleaching Recovery Kinetics. Biophysical Journal 16, 1055-1069.

Axelrod, D., Ravdin, P., Koppel, D.E., Schlessinger, J., Webb, W.W., Elson, E.L., Podleski, T.R., 1976b. Lateral Motion of Fluorescently Labeled Acetylcholine Receptors in Membranes of Developing Muscle-Fibers. Proceedings of the National Academy of Sciences of the United States of America 73, 4594-4598.

Banks, D.S., Fradin, C., 2005. Anomalous diffusion of proteins due to molecular crowding. Biophysical Journal 89, 2960-2971.

Benichou, O., Chevalier, C., Klafter, J., Meyer, B., Voituriez, R., 2010. Geometry-controlled kinetics. Nature chemistry 2, 472-477.

Berg, O.G., Winter, R.B., von Hippel, P.H., 1981. Diffusion-driven mechanisms of protein translocation on nucleic acids. 1. Models and theory. Biochemistry 20, 6929-6948.

Berkovich, R., Wolfenson, H., Eisenberg, S., Ehrlich, M., Weiss, M., Klafter, J., Henis, Y.I., Urbakh, M., 2011. Accurate Quantification of Diffusion and Binding Kinetics of Non-integral Membrane Proteins by FRAP. Traffic 12, 1648-1657.

Berry, H., 2002. Monte Carlo simulations of enzyme reactions in two dimensions: Fractal kinetics and spatial segregation. Biophysical Journal 83, 1891-1901.

Bouchaud, J.P., Georges, A., 1990. Anomalous Diffusion in Disordered Media - Statistical Mechanisms, Models and Physical Applications. Physics Reports-Review Section of Physics Letters 195, 127-293.

Brauchle, C., Lamb, D.C., Michaelis, J., 2009. Single particle tracking and single molecule energy transfer. Wiley-VCH, Weinheim.

Brockmann, D., Hufnagel, L., Geisel, T., 2006. The scaling laws of human travel. Nature 439, 462-465.

Dertinger, T., Pacheco, V., von der Hocht, I., Hartmann, R., Gregor, I., Enderlein, J., 2007. Two-focus fluorescence correlation spectroscopy: a new tool for accurate and absolute diffusion measurements. Chemphyschem 8, 433-443.

Digman, M.A., Gratton, E., 2011. Lessons in fluctuation correlation spectroscopy. Annual review of physical chemistry 62, 645-668.

Dix, J.A., Verkman, A.S., 2008. Crowding effects on diffusion in solutions and cells. Annual review of biophysics 37, 247-263.

Einstein, A., 1905. Über die von der molekularkinetischen Theorie der Wärme geforderte Bewegung von in ruhenden Flüssigkeiten suspendierten Teilchen. Annalen der Physik 322, 549-560.

Ellis, R.J., Minton, A.P., 2003. Cell biology: join the crowd. Nature 425, 27-28.
Elsner, M., Hashimoto, H., Simpson, J.C., Cassel, D., Nilsson, T., Weiss, M., 2003. Spatiotemporal dynamics of the COPI vesicle machinery. Embo Reports 4, 1000-1005.

Engelman, D.M., 2005. Membranes are more mosaic than fluid. Nature 438, 578-580.

Ernst, D., Hellmann, M., Kohler, J., Weiss, M., 2012. Fractional Brownian motion in crowded fluids. Soft Matter 8, 4886-4889.

Frick, M., Schmidt, K., Nichols, B.J., 2007. Modulation of lateral diffusion in the plasma membrane by protein density. Curr Biol 17, 462-467.

Fujiwara, T., Ritchie, K., Murakoshi, H., Jacobson, K., Kusumi, A., 2002. Phospholipids undergo hop diffusion in compartmentalized cell membrane. The Journal of cell biology 157, 1071-1081.

Goehring, N.W., Chowdhury, D., Hyman, A.A., Grill, S.W., 2010. FRAP analysis of membrane-associated proteins: lateral diffusion and membrane-cytoplasmic exchange. Biophys J 99, 2443-2452.

Golding, I., Cox, E.C., 2006. Physical nature of bacterial cytoplasm. Physical Review Letters 96.

Gonzalez, M.C., Hidalgo, C.A., Barabasi, A.L., 2008. Understanding individual human mobility patterns. Nature 453, 779-782.

Goulian, M., Simon, S.M., 2000. Tracking single proteins within cells. Biophys J 79, 2188-2198.

Griffiths, G., Warren, G., Quinn, P., Mathieu-Costello, O., Hoppeler, H., 1984. Density of newly synthesized plasma membrane proteins in intracellular membranes. I. Stereological studies. The Journal of cell biology 98, 2133-2141.

Guigas, G., Kalla, C., Weiss, M., 2007a. The degree of macromolecular crowding in the cytoplasm and nucleoplasm of mammalian cells is conserved. Febs Letters 581, 5094-5098.

Guigas, G., Kalla, C., Weiss, M., 2007b. Probing the nanoscale viscoelasticity of intracellular fluids in living cells. Biophysical Journal 93, 316-323.

Guigas, G., Weiss, M., 2006. Size-dependent diffusion of membrane inclusions. Biophysical Journal 91, 2393-2398.

Guigas, G., Weiss, M., 2008. Sampling the cell with anomalous diffusion - The discovery of slowness. Biophysical Journal 94, 90-94.

Havlin, S., Benavraham, D., 1987. Diffusion in Disordered Media. Advances in Physics 36, 695-798.

He, Y., Burov, S., Metzler, R., Barkai, E., 2008. Random time-scale invariant diffusion and transport coefficients. Physical Review Letters 101.

Hellmann, M., Heermann, D.W., Weiss, M., 2011. Anomalous reaction kinetics and domain formation on crowded membranes. EPL 94, 5.

Hellmann, M., Heermann, D.W., Weiss, M., 2012. Enhancing phosphorylation cascades by anomalous diffusion. Epl 97.

Hoefling, F., Franosch, T., 2013. Anomalous transport in the crowded world of biological cells. Reports on Progress in Physics 76, 046602.

Hofling, F., Franosch, T., Frey, E., 2006. Localization transition of the three-dimensional lorentz model and continuum percolation. Phys Rev Lett 96, 165901.

Hughes, B.D., Pailthorpe, B.A., White, L.R., Sawyer, W.H., 1982. Extraction of membrane microviscosity from translational and rotational diffusion coefficients. Biophys J 37, 673-676.

Humphries, N.E., Queiroz, N., Dyer, J.R.M., Pade, N.G., Musyl, M.K., Schaefer, K.M., Fuller, D.W., Brunnschweiler, J.M., Doyle, T.K., Houghton, J.D.R., Hays, G.C., Jones, C.S., Noble, L.R., Wearmouth, V.J., Southall, E.J., Sims, D.W., 2010. Environmental context explains Levy and Brownian movement patterns of marine predators. Nature 465, 1066-1069.

Kholodenko, B.N., 2006. Cell-signalling dynamics in time and space. Nature Reviews Molecular Cell Biology 7, 165-176.

Klafter, J., Shlesinger, M.F., Zumofen, G., 1996. Beyond Brownian motion. Physics Today 49, 33-39.

Klafter, J., Sokolov, I.M., 2012. First steps in random walks : from tools to applications. Oxford University Press, Oxford ; New York.

Kolin, D.L., Wiseman, P.W., 2007. Advances in image correlation spectroscopy: measuring number densities, aggregation states, and dynamics of fluorescently labeled macromolecules in cells. Cell biochemistry and biophysics 49, 141-164.

Kopelman, R., 1988. Fractal Reaction-Kinetics. Science 241, 1620-1626.

Lippincott-Schwartz, J., Snapp, E., Kenworthy, A., 2001. Studying protein dynamics in living cells. Nature reviews 2, 444-456.

Lubelski, A., Klafter, J., 2009. Fluorescence correlation spectroscopy: the case of subdiffusion. Biophys J 96, 2055-2063.

Lubelski, A., Sokolov, I.M., Klafter, J., 2008. Nonergodicity mimics inhomogeneity in single particle tracking. Physical Review Letters 100.

Magde, D., Webb, W.W., Elson, E., 1972. Thermodynamic Fluctuations in a Reacting System - Measurement by Fluorescence Correlation Spectroscopy. Physical Review Letters 29, 705-&.

Malchus, N., Weiss, M., 2010. Anomalous Diffusion Reports on the Interaction of Misfolded Proteins with the Quality Control Machinery in the Endoplasmic Reticulum. Biophysical Journal 99, 1321-1328.

Mandelbrot, B., van Ness, J.W., 1968. Fractional Brownian motions, fractional noises and applications. SIAM Review 10, 422-437.

Mandelbrot, B.B., 1983. The fractal geometry of nature, Updated and augmented. ed. W.H. Freeman, San Francisco.

Markevich, N.I., Hoek, J.B., Kholodenko, B.N., 2004. Signaling switches and bistability arising from multisite phosphorylation in protein kinase cascades. The Journal of cell biology 164, 353-359.

Mason, T.G., Weitz, D.A., 1995. Optical Measurements of Frequency-Dependent Linear Viscoelastic Moduli of Complex Fluids. Physical Review Letters 74, 1250-1253.

McGuffee, S.R., Elcock, A.H., 2010. Diffusion, crowding & protein stability in a dynamic molecular model of the bacterial cytoplasm. PLoS computational biology 6, e1000694.

Meinhardt, H., 1982. Models of biological pattern formation. Academic Press, London ; New York.

Pan, W.C., Filobelo, L., Pham, N.D.Q., Galkin, O., Uzunova, V.V., Vekilov, P.G., 2009. Viscoelasticity in Homogeneous Protein Solutions. Physical Review Letters 102.

Petrov, E.P., Schwille, P., 2008. Translational diffusion in lipid membranes beyond the Saffman-Delbruck approximation. Biophys J 94, L41-43.

Quinn, P., Griffiths, G., Warren, G., 1984. Density of newly synthesized plasma membrane proteins in intracellular membranes II. Biochemical studies. The Journal of cell biology 98, 2142-2147.

Rigler, R., Elson, E., 2001. Fluorescence correlation spectroscopy : theory and applications. Springer, Berlin ; New York.
Rudnick, J., Gaspari, G., 1987. The Shapes of Random-Walks. Science 237, 384-389.

Saffman, P.G., Delbruck, M., 1975. Brownian motion in biological membranes. Proc Natl Acad Sci U S A 72, 3111-3113.

Saxton, M.J., 1996. Anomalous diffusion due to binding: a Monte Carlo study. Biophys J 70, 1250-1262.

Saxton, M.J., 2001. Anomalous subdiffusion in fluorescence photobleaching recovery: a Monte Carlo study. Biophys J 81, 2226-2240.

Saxton, M.J., 2002. Chemically limited reactions on a percolation cluster. Journal of Chemical Physics 116, 203-208.

Saxton, M.J., 2007. A biological interpretation of transient anomalous subdiffusion. I. Qualitative model. Biophys J 92, 1178-1191.

Seksek, O., Biwersi, J., Verkman, A.S., 1997. Translational diffusion of macromolecule-sized solutes in cytoplasm and nucleus. The Journal of cell biology 138, 131-142.

Sims, D.W., Southall, E.J., Humphries, N.E., Hays, G.C., Bradshaw, C.J.A., Pitchford, J.W., James, A., Ahmed, M.Z., Brierley, A.S., Hindell, M.A., Morritt, D., Musyl, M.K., Righton, D., Shepard, E.L.C., Wearmouth, V.J., Wilson, R.P., Witt, M.J., Metcalfe, J.D., 2008. Scaling laws of marine predator search behaviour. Nature 451, 1098-U1095.

Smoluchowski, M.V., 1916. Drei Vorträge über Diffusion, Brownsche Molekularbewegung und Koagulation von Kolloidteilchen. Phys. Z. 17, 557-571.

Soumpasis, D.M., 1983. Theoretical analysis of fluorescence photobleaching recovery experiments. Biophys J 41, 95-97.

Stiehl, O., Weiss, M., 2013. Kinetics of conformational fluctuations in DNA hairpin-loops in crowded fluids. submitted.

Szymanski, J., Weiss, M., 2009. Elucidating the Origin of Anomalous Diffusion in Crowded Fluids. Physical Review Letters 103, 4.

Takahashi, K., Tanase-Nicola, S., ten Wolde, P.R., 2010. Spatio-temporal correlations can drastically change the response of a MAPK pathway. Proc Natl Acad Sci U S A 107, 2473-2478.

Thompson, M.A., Lew, M.D., Moerner, W.E., 2012. Extending Microscopic Resolution with Single-Molecule Imaging and Active Control. Annual Review of Biophysics, Vol 41 41, 321-342.

Tolic-Norrelykke, I.M., Munteanu, E.L., Thon, G., Oddershede, L., Berg-Sorensen, K., 2004. Anomalous diffusion in living yeast cells. Physical Review Letters 93.

Tomishige, M., Kusumi, A., 1999. Compartmentalization of the erythrocyte membrane by the membrane skeleton: intercompartmental hop diffusion of band 3. Molecular biology of the cell 10, 2475-2479.

Tseng, Y., Kole, T.P., Wirtz, D., 2002. Micromechanical mapping of live cells by multiple-particle-tracking microrheology. Biophysical Journal 83, 3162-3176.

Wachsmuth, M., Waldeck, W., Langowski, J., 2000. Anomalous diffusion of fluorescent probes inside living cell nuclei investigated by spatially-resolved fluorescence correlation spectroscopy. Journal of molecular biology 298, 677-689.

Weber, S.C., Spakowitz, A.J., Theriot, J.A., 2010. Bacterial Chromosomal Loci Move Subdiffusively through a Viscoelastic Cytoplasm. Physical Review Letters 104.

Weigel, A.V., Simon, B., Tamkun, M.M., Krapf, D., 2011. Ergodic and nonergodic processes coexist in the plasma membrane as observed by single-molecule tracking. Proc Natl Acad Sci U S A 108, 6438-6443.

Weiss, M., 2003. Stabilizing Turing patterns with subdiffusion in systems with low particle numbers. Physical Review E 68.

Weiss, M., 2004. Challenges and artifacts in quantitative photobleaching experiments. Traffic 5, 662-671.

Weiss, M., Elsner, M., Kartberg, F., Nilsson, T., 2004. Anomalous subdiffusion is a measure for cytoplasmic crowding in living cells. Biophysical Journal 87, 3518-3524.

Weiss, M., Hashimoto, H., Nilsson, T., 2003. Anomalous protein diffusion in living cells as seen by fluorescence correlation spectroscopy. Biophysical Journal 84, 4043-4052.

Yamada, S., Wirtz, D., Kuo, S.C., 2000. Mechanics of living cells measured by laser tracking microrheology. Biophysical Journal 78, 1736-1747.

Zhou, H.X., Rivas, G., Minton, A.P., 2008. Macromolecular crowding and confinement: biochemical, biophysical, and potential physiological consequences. Annual review of biophysics 37, 375-397.

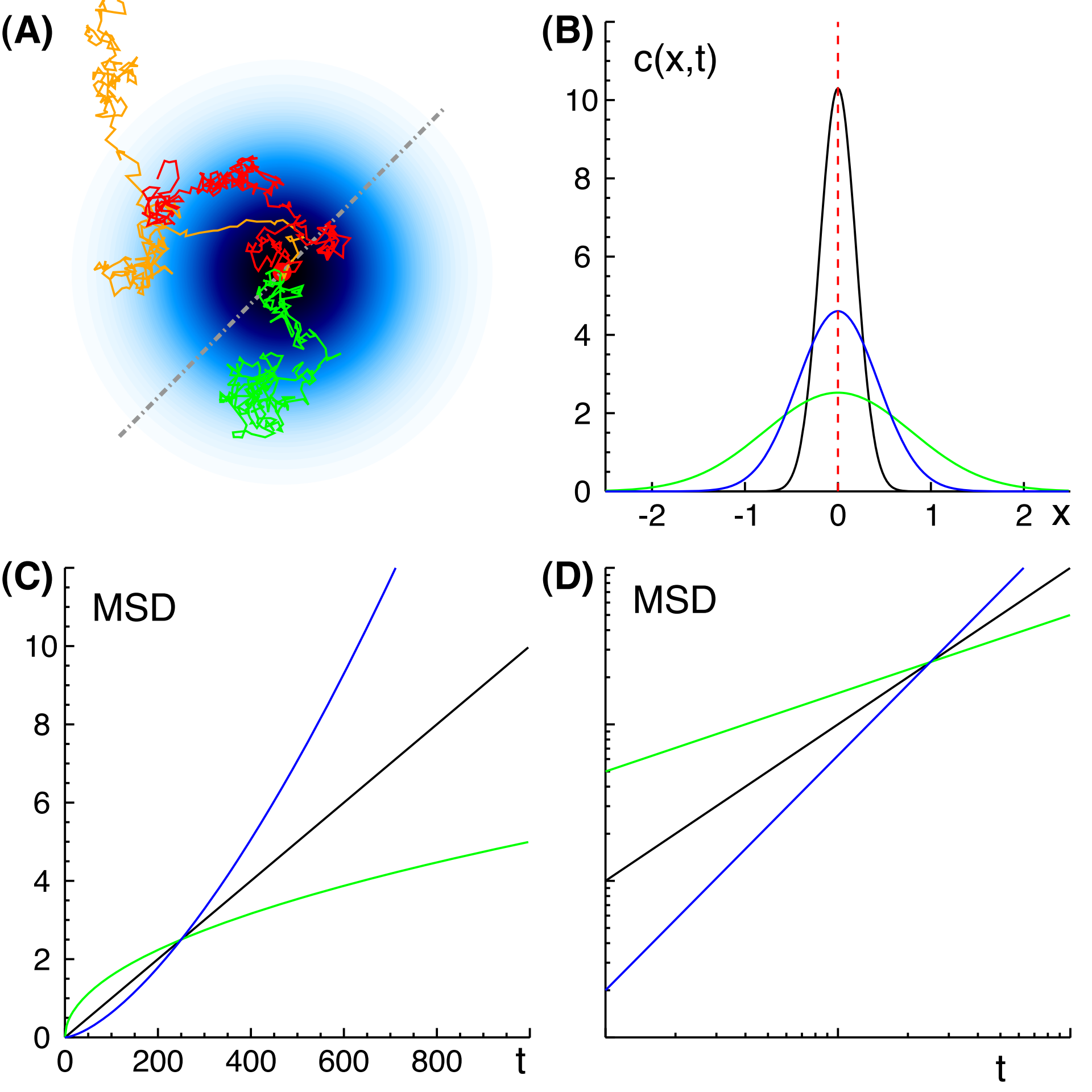
(A)
(B)
c(x,t)
10
8
6
4
2
0
-2
-1
0
1
2
x
(C)
MSD
10
8
6
4
2
0
0
200
400
600
800
t
(D)
MSD
t

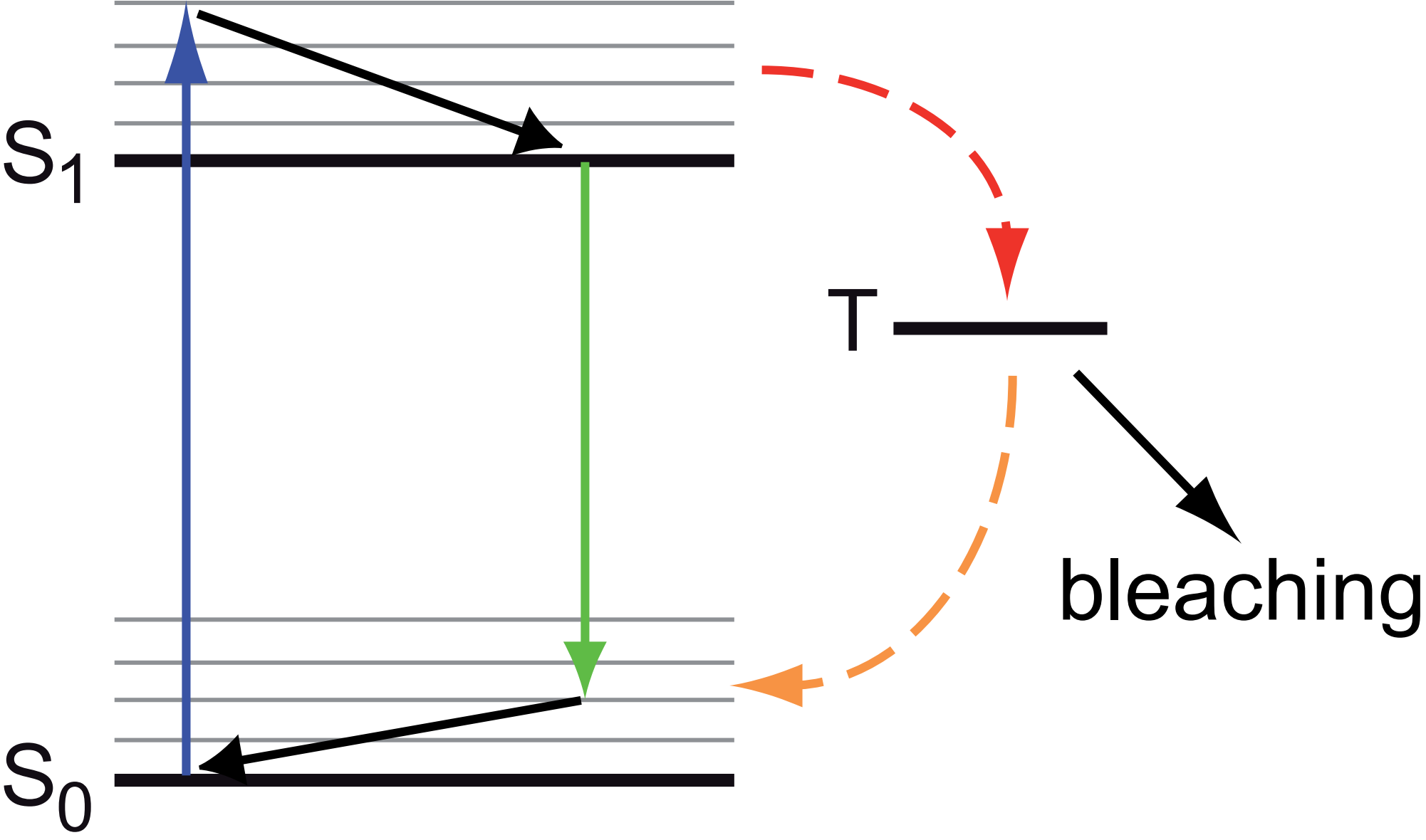
S1
T
bleaching
S0

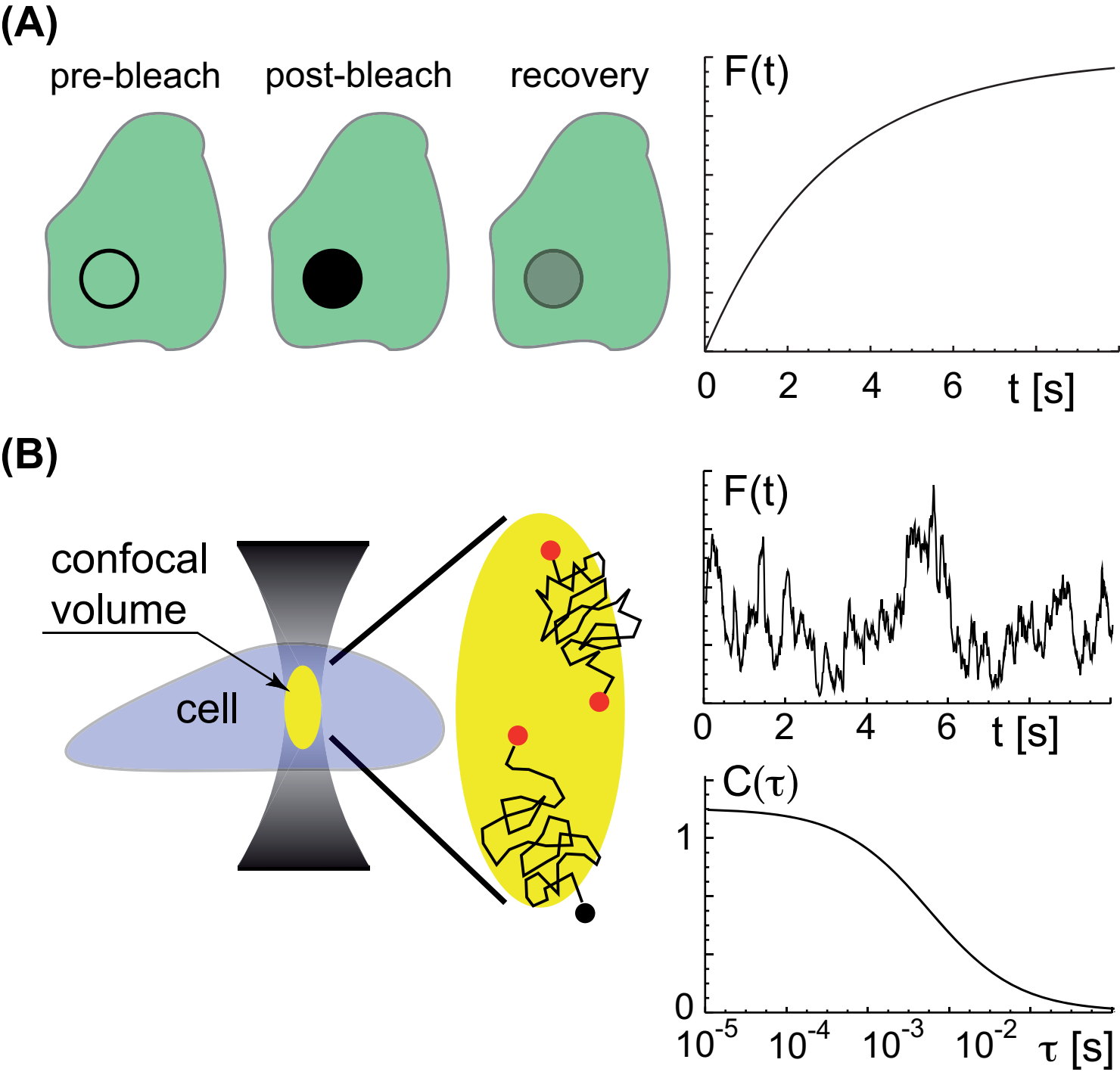
(A)
pre-bleach
post-bleach
recovery
F(t)
0
2
4
6
t [s]
(B)
confocal
volume
cell
F(t)
0
2
4
6
t [s]
C(τ)
1
0
10-5
10-4
10-3
10-2
τ [s]

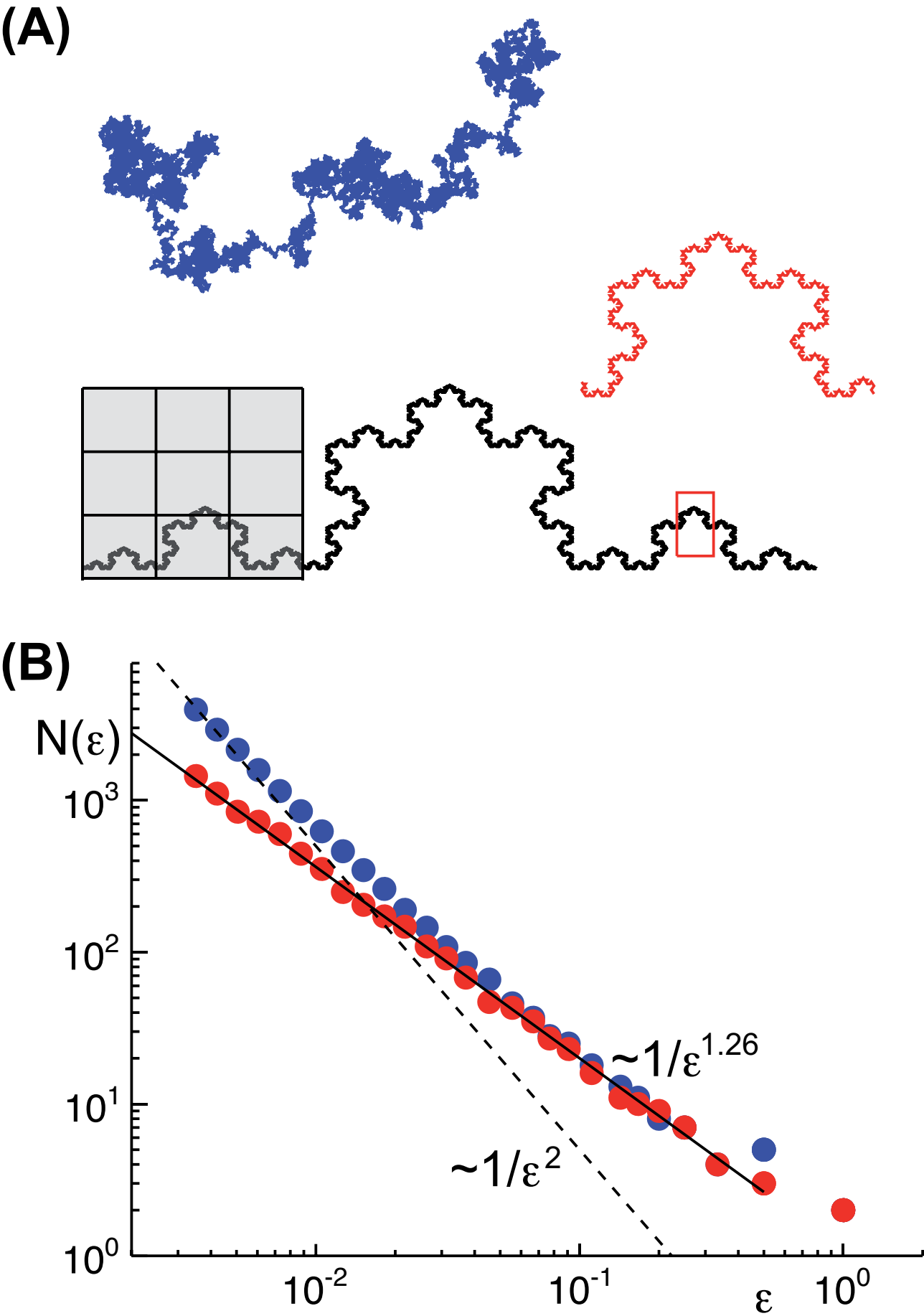
(A)
(B)
N(ε)
10^3
10^2
10^1
10^0
10^-2
10^-1
ε
10^0
~1/ε^1.26
~1/ε^2